Construction and Building Materials 240 (2020) 117962

Contents lists available at ScienceDirect

Construction and Building Materials

journal homepage: www.elsevier.com/locate/conbuildmat

Effect of high metakaolin content on compressive and shear-bond strengths of oil well cement at 80 °C

Petro Ezekiel Mabeyo [a,b], Yusra Salmin Ibrahim [a], Jun Gu [a,*]

[a] Department of Petroleum Engineering, Faculty of Earth Resources, China University of Geosciences, Wuhan 430074, China
[b] Department of Chemistry, Faculty of Science, Dar es Salaam University College of Education, P. O. Box 2329, Dares Salaam, Tanzania

HIGHLIGHTS

- The effect of varied metakaolin dosage on the cementitious system was investigated.
- Metakaolin increased the compressive and shear bond strengths.
- Higher metakaolin content showed deceleration of cement hydration at an early age.
- The binary system presented a high potential for a strong cement-formation bond.
- A better proportion of metakaolin with better performance was proposed.

ARTICLE INFO

Article history:
Received 6 October 2019
Received in revised form 22 December 2019
Accepted 24 December 2019

Keywords:
Metakaolin
Compressive strength
Shear bond strength
Oil well cement
Supplementary cementitious materials

ABSTRACT

This paper reports the effect of high metakaolin content on compressive and shear bond strengths of oil well cement cured at 80 °C. X-ray diffraction (XRD), and thermo gravimetric-differential scanning calorimetry (TG-DSC) used to study cement phases. Both compressive and shear bond strengths increased with hydration age. The binary system with 20% metakaolin displayed better compressive strength relative to the neat oil well cement samples. It increased by 17 and 20% at 3 and 28 days of hydration, respectively. The shear bond strength equally increased by 145 and 56% at 3 and 28 days, respectively. The results of this study, therefore, point to a feasible cement system for the long life of the oil and gas wells.

1. Introduction

One of the principal objectives of oil well primary cementing is providing complete and permanent annular-zonal isolations. This includes isolations from mechanical and chemical stresses. The isolation prevents the exchange of fluids between zones within reservoirs or between separate reservoirs during shut-ins [1,2]. Bonding of cement to casing pipe and formation is critical to the success of oil and gas well cementing. The strength of cement sheath and bond at the interfaces is significant for the long life of oil and gas well [3]. The latter draws attention to the study of shear bond strength (SBS) with improved oil well cement (OWC) properties. It is an important property of cement and other binders used in oil and gas well construction activities. De-bonding at the interface of casing-cement-formation in the long term is a result of lower bond strength. It occurs when more dynamic loads are introduced into the well. The latter allows the flow of formation fluids from one zone to another. Fluids can further flow to the surface resulting in health and safety risks. Consequently, to prevent leakage paths at this boundary higher bond strength is anticipated [2,4]. Therefore, a strong bond between cement and casing implies the long-term integrity of the wellbore [5].

The quality of cement used in well cementing, drilling fluids and type of drilling fluids affect the cement-formation bond. The effect of the fluids is normally by decreasing the bonding strength. Some research works have introduced technologies of converting mud cake into cementitious material to improve the cement-formation bond strength. These technologies include; mud to cement (MTC) [6], mud cake to agglomerated cake (MTA) [7,8] and mud cake solidification (MCS) [9,10]. Except for MTC which is challenged, due to the shrinkage and cracking caused by the brittle nature of the MTC solidified body [10], the rest have presented good results on SBS. Nevertheless, the quality of cement

* Corresponding author.
E-mail address: gujun@cug.edu.cn (J. Gu).

https://doi.org/10.1016/j.conbuildmat.2019.117962
0950-0618/

can significantly increase the bond strength at the interface. When subjected to subsurface temperature and pressure, the physical and chemical properties of Portland-based cement change significantly [11]. Its brittleness and volume shrinkage can cause of cement failure under subsurface conditions [12,13]. However, the use of supplementary cementitious materials (SCM) has been proposed to replace some amount of cement for properties improvement.

SCM is used in cement as an important material that controls both the physical and chemical properties of fresh and hydrated cementitious systems. Their mineral and chemical compositions are necessary for partial replacement of cement. On the other hand, supplementing ordinary Portland cement (OPC) significantly reduces the problem of CO_2 emission. It further mitigates the disposal of a variety of industrial byproducts such as silica fumes, fly-ash, ground granulated blast furnace slags, electric arc furnace slag, ceramic wastes and lime-rich slugs [14–19]. One of the reported SCM which the current study has focused on is Metakaolin, $Al_2Si_2O_7$ (MK). It is produced from calcination of kaolin at temperatures of approximately 500–800 °C [20–24]. The temperature is much lower compared to 1450 °C required to produce OPC [25]. Its production also releases little CO_2 compared to cement production. MK is highly reactive SCM and rich in alumina and silica content [26]. High proportions of these contents help to reduce calcium to silica ratio (Ca/Si); which is significant in cement mechanical strength improvement. Its chemical properties have been compared to OPC and found to be suitable as OPC partial replacement for high strength concrete [27,28]. MK enhances property development in the MK-OPC system through the filler effect as well as a pozzolanic reaction [29,30]. It further prevents cement from acidic fluids attack [31,32].

Like in the concrete industry some reports are available on OWC property improvement using MK. It is reported to be suitable for deep well, geothermal well and acid-rich well cementing [18,33,34]. However, none of these researches have studied SBS with a specific focus at the cement-formation interface. Most of the reported studies on SBS of cement concentrated on the cement-to-casing interface [2,35–37]. They highlighted more of the necessary features needed to have a strong bond at the cement-casing interface. Some of these studies concluded that roughness of the casing pipe and good initial removal of mud leads to improved SBS [36,37]. Recently, Hwang et al. [2] have employed the use of up to 35% of silica flour as SCMs targeting the acidic environment while the rest used conventional OWC in their studies.

The optimum amount of MK suitable to provide significant strength evolution is still a subject of discussion. Different conclusions have been drawn amongst reported works in the concrete and oil and gas industry. Some studies in concrete reported the use of MK content between 5 and 25% [32,38–41]. They point to low content to being suitable for concrete strength evolution. Dinakar et al. [39] incorporated the binary cement system with 5–15% wt. of MK. Their conclusion favored 10% wt. as an optimum level for concrete strength evolution in terms of compressive strength. This report is in agreement with the reported work by Ramezanianpour and Bahrami Jovein [41]; though the water to cement ratios are 0.3 and 0.35 and curing temperatures of 27 and 23 °C, respectively. Replacement of cement with 8% wt. MK in concrete is also reported to have a catalytic effect on early cement hydration. This occurs through enhancing cementitious phases dissolution that provides well-dispersed sites for nucleation of the hydration products [38]. Weng et al. [40] reported on the mechanical properties of cement with 5–25% wt. of MK. They observed that MK improved the compressive strength of cement mortar while content beyond 20% wt. had a detrimental effect on strength and efflorescence. The latter agrees in part by El-Diadamony et al. who reported 20% wt. MK to be suitable for accelerating water consistency, initial setting times and compressive strength of MK-blended cement pastes [42].

Some reports on higher MK dosage at higher temperatures are also available. Bu et al. [34] studied the replacement of cement with MK content at higher temperatures. They found that a high dosage had good strength evolution at the temperature of 150 °C and above. From the cited studies, it is seen that apart from curing age, temperature influences the amount of MK suitable for cement property improvement. The latter agrees with Morsy et al. [43] who reported that replacement of cement with 5% wt. nano-MK at low temperature (25 °C) leads to optimal mortar. Further replacement with 15% wt. nano-MK at elevated temperature above 250 °C gives good results. However, studies on oil well cementation incorporating a high dosage of MK at normal oil well temperature with more emphasis on the cement-formation are scarcely reported. Using higher MK content could be significant to cement property improvement as well as environmental concerns in cement production. Therefore, this research paper studied the effect of up to 40% wt. MK on CS and SBS of OWC at 80 °C. The SBS studies focus on the cement-formation interface by using simulated wellbores (SWBs).

2. Experimental program

Compressive and shear bond strengths tests were carried out for both OWC with and without MK at the Cement and Well Completion Laboratory in the Department of Petroleum Engineering, China University of Geosciences (Wuhan).

2.1. Materials

Commercial API Class G oil well cement was used throughout this study. Metakaolin SP33, a BASF™ product used as received for partial replacement of OWC was obtained from Qingdao Topsen Chem. Co, LTD (Qingdao, China). The chemical composition of MK and OWC are presented in Table 1. To take care of the high water demand due to MK, a dispersant made of polymerized and modified Methanal and Acetone from Henan Xinxiang No.7 Chemical Co., Ltd (Henan, China) was used during slurry preparation to reduce the friction between particles. Water-based drilling mud obtained from Jianghan oilfield (Jianghan, China) was used to simulate the mud cake formation in the simulated wellbore. High-temperature butter was used to mount the glass slab on one end of the SWB for better placement of mud and letter the cement slurry. A glass rod was then used to remove the fluffy mud cake

Table 1
Chemical Composition and Physical Properties of OWC and MK.

Oxides (%)										Density (g/cm^3)	SSA (m^2/g)	L.O.I
	CaO	SiO_2	Fe_2O_3	Al_2O_3	SO_3	MgO	Na_2O	K_2O	TiO_2			
OWC	64.20	19.40	5.50	4.50	2.80	2.00	0.10	0.60	–	3.15	0.336	0.49
MK	0.03	52.30	0.60	44.60	–	0.04	0.20	0.15	1.70	2.59	40.000	0.45

Table 2
Composition of OWC pastes with MK.

Mixes (%)		Abbreviation	OWC (g)	MK (g)	Water/Binder ratio	Dispersant (%Wt. MK)
OWC	MK					
100	–	MK0	792.00	–	0.45	–
90	10	MK10	712.80	79.20	0.45	0.50
80	20	MK20	633.60	158.40	0.45	1.00
70	30	MK30	554.40	237.60	0.45	1.50
60	40	MK40	475.20	316.80	0.45	2.00

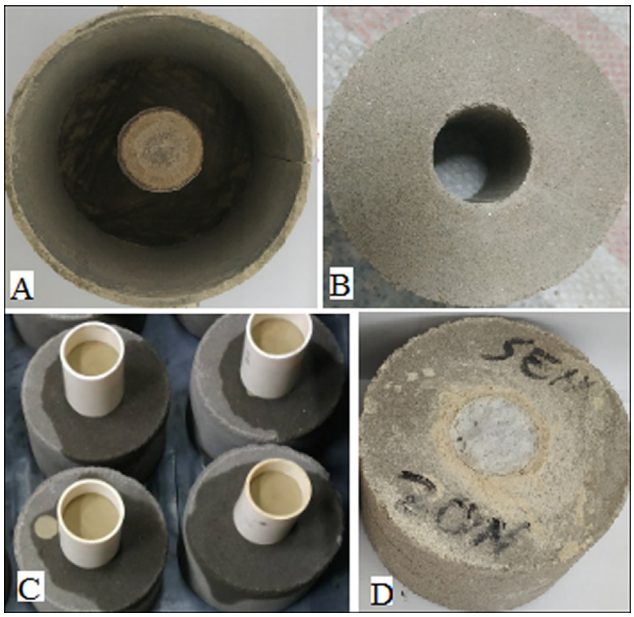

Fig. 1. Experimental Samples: A-PVC assemblage for SWB preparation; B-Dried SWB; C-SWB with water-based mud to simulate mud cake formation; D-SWB with hardened cement paste ready for SBS test.

and level the cake to the thickness of about 0.5 mm in the range as required for cases of oil and gas wells in China [44].

2.2. Methods

2.2.1. Slurry preparation

Cement slurries were prepared according to API 10A [45] specifications with water to binder ratio of 0.45. Table 2 presents the composition of each experimental mix system. The weighed amount of cement and admixtures were hand mixed in the dry bowl using a clean spatula. The dispersant was subsequently dissolved into the mixing water. The mixing aqueous solution was then poured into the blender. The mixing was initiated slowly and then the cement admixture added for 15 s while blending at a slow speed of 4000 rpm. The manual mixing undertaken for 30 s with the rubber spatula facilitating recovery of the material sticking to the wall of the mixing container, to ensure homogeneity. Then to finalize, the cover was placed on the mixing container and mixing was done at a high speed of 12000 rpm for 35 s.

2.2.2. Compressive strength

To determine the behavior of the hydrated cement under the compressive load, the CS test was done to all cured sample mixes. The prepared cement slurries were placed into several molds with equal side dimensions of 5 cm. The slurries were compressed using the mold cover plates to release existing gas bubbles. Four cubes were prepared for each mixing ratio and subjected to curing at a temperature of 80 °C for 3, 7, 14 and 28 days. Curing of samples at the selected temperature was done in conformity with API PR 10B-2 recommended practices procedures [46]. After reaching the curing time, three cubes of each kind of the hydrated cement sheath were removed from the water bath, wiped to remove loose solids on the sample surface and compressed using unconfined compressive strength tester. The compression was done at the pressures required to crack the sample. A compressive load (kN) was recorded for each of the three samples. The average values were recorded and converted to compressive strength (MPa), according to the equation; $p = 10F/A$, where p is compressive strength, F is loading force (kN), A is the area of the cube acted by the loading force (cm^2) and 10 is the unit conversion factor. The fourth cube was ground into powder for XRD and TG-DSC studies.

2.2.3. Simulation of wellbores

Previous studies on cement bonds have shown that the strength of cement bond on cement-formation or casing-cement depends on the nature of the contact surfaces, cement type, the hydration characteristics of the cement and curing time [5,35]. It is therefore important to ensure good condition for the formation surface before slurry placement to maintain the seal at the cement-to-formation interface [47]. To meet this requirement, it was necessary to carefully prepare the experimental sample based on the tested procedures (Fig. 1). The mortar for preparing the SWBs was made from well-sorted sand and cement. The materials were mixed thoroughly at the cement to the sand ratio of 0.37, then the mortar was made with water to a solid ratio of 0.0875. The preparation of the SWBs was partly done according to the reported procedures [44]. The mortar was placed in the adjustable PVC pipe with an internal diameter of 100 mm. A steel casing with an external diameter of 33 mm was placed at the center of the assembled PVC to simulate the wall after placing the mortar paste. Then, the mortar was placed uniformly on the pressure testing machine frame. The surface of the mixed materials was pressed slowly and gradually compressed to 10kN with the steely cylindrical indenter at a rate of 0.04 kN/s. The pressure was then released to facilitate the extraction of the compressed mortar with its PVC. The SWB was left to dry at room temperature for 72 h before removing the adjustable PVC pipe mold to separate from the prepared SWB.

To allow injection of the fluids, each of the SWBs was mounted on a glass plate to seal the base with high-temperature butter. The SWBs were injected with water-based drilling mud to simulate mud cake formation before injection of the designed oilwell cement slurry. Injection of drilling fluids and later the slurry into the SWBs were partly done according to Gu et al. [8,44]. Drilling fluid was injected into SWBs to thoroughly fill the whole annular space and left for 4 h to allow a mud cake formation. The fluffy mud cake was gradually removed with glass rods to simulate the activity of bore until a dense mud cake of about 0.5 mm was formed. SWBs with leveled mud cake was mounted on the glass plate to seal and allow injection of the cement slurry. The prepared cement slurry, with the appropriate replacements with MK, was injected into the SWBs with uniform mud cake thickness. A stirrer

rod was used to stir the cement slurry several times to ensure consistency. The slurry filled SWBs were put into the curing bath for 3, 7, 14 and 28 days at 80 °C. Finally, the test of shear force at the cement interface was done after the height of each cured SWBs was recorded.

2.2.4. Shear bond strength test

The study of the SBS was done by hydraulic compression tester [5]. The hydraulic press was adjusted to ensure the specimen fits between its force plate and backing plate (Fig. 2). The hydrated sheath of the cured test sample was leveled to allow the force head to fit well and then placed between the loading plates for the SBS test. A loading force was then applied to the specimen at a uniform rate. A metal force head with a diameter of 31 mm (less by 2 mm to the bore diameter of the SWB was used to press the hydrated cement sheath from the SWB. The maximum force reached when the shear bond just breaks, was recorded and used to determine the shear bond strength. Three samples were tested for each curing age and mix ratios. The average of the three recorded readings was used to calculate the shear bond strengths according to Equation $p = 10F/\pi hD$ [44], where p is shear bond strength (MPa), F is the relief force at the cement-interlayer interface (kN), h is the height of SWB (cm), and D is the inner (bore) diameter of SWB (cm).

2.2.5. X-ray diffraction (XRD) analyses

To identify mineral phases present in hydrated cement samples, D8 Advance XRD (Bruker D8 Advance, Germany) was used. The instrument is equipped with a LynxEye detector and graphite-monochromatized CuKα radiation source. The radiations were generated at the voltage of 40 kV and current of 40 mA. The CuKβ was filtered with Ni-filter. 0.5 g of finely grounded dry samples were used to obtain the XRD patterns. FT scanning was carried out at 2θ in a range of 5–90° while the step size was 0.01°. MDI Jade (version 6.5) software was used for XRD raw data processing, pattern quantification, and identification. The test was carried out at the College of Material and Chemical Engineering, the Future City Campus of China University of Geosciences (Wuhan).

2.2.6. Thermo gravimetric-differential scanning calorimetry- (TG-DSC)

TG-DSC was used to study the phase composition of the hydrated OWC samples with and without MK. The STA 409 PC model (NETZSCH Instruments Manufacturing Co., Ltd, Germany) TG-DSC analyzer was used for carrying out the studies of the hydration degree in the mixture of MK and oil well cement slurry. TG simultaneously measured the weight loss due to the decompositions while the ranges corresponding to thermal decompositions of different phases in samples were located by DSC. TG-DSC tests were performed by heating from 30 °C to 1150 °C at an increasing temperature rate of 20 °C/min. The test was carried out under a nitrogen atmosphere at the flow rate of 50 mL/min. Samples for TG-DSC were dried at 105 °C for 24 h and ground to a fine powder; before analysis. About 30 mg of powdered samples were put into an aluminum oxide crucible for each test. The test was done at the College of Material and Chemical Engineering, the Future City Campus of China University of Geosciences (Wuhan).

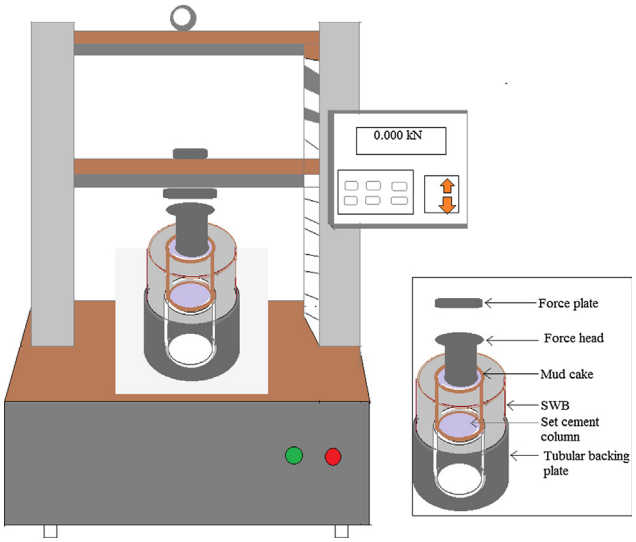

Fig. 2. Sketch of SBS Measuring Apparatus.

3. Test results and discussion

3.1. Slurry consistency

Cement slurry for the mixes containing MK showed high water demand and reduced flow ability. The water demand increased with the amount of MK replacing OWC. Keeping water to binder ratio of 0.45 as a constant to all mixed proportions demanded the use of dispersant. The amount of dispersant varied directly proportionally with the amount of MK for slurry consistency. Table 2 presents the proportion of dispersant for each binary system.

3.2. Compressive strength

Fig. 3 presents the compressive strength of OWC with and without MK cured at 80 °C for 3, 7, 14 and 28 days. The figure shows that the variations of CS for both neat OWC (MK0) and binary systems have the same trend. The CS increased with curing age for all experimental samples. The strength evolution for MK0 was attributable to the products of cement hydration. C-S-H contributes more to the strength than does CH. It was also observed that CS did not vary in direct proportionality to the amount of MK replacing OWC. This was evident for MK40 which presented lower CS than MK20 and MK30, especially for early hydration age. While it was expected to have more strength at 3 days of cement curing of samples with higher MK content due to filler effect and pozzolanic reaction, the results point to the opposite. The observation is attributable to several reasons. The first reason could be that the dissolution of higher MK content releases Aluminate ions. The ions subsequently adsorb onto the surface of cement, acting as nucleation and hydration inhibitor until later ages [48–50]. Inhibition of the filler effect on hydration then leads to poor solid-to-solid connectivity within the cement microstructure since no pronounced C-S-H addition, as a result, no sufficient increase in CS [14,51]. The second possible reason is the dilution effect. High

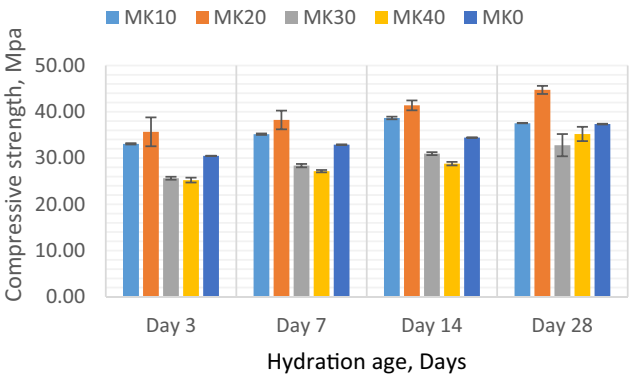

Fig. 3. Compressive strength for different mixes at 3, 7, 14, and 28 days curing ages.

metakaolin content dilutes the cement thereby reducing the content of cement available for hydration. Low cement content due to the dilution effect results in fewer hydration products. Fewer hydration products especially C-S-H leads to reduced strength evolution. Fewer CH negatively affects the production of secondary C-S-H from the pozzolanic reaction between CH and MK. Therefore, the dilution effect compromises strength evolution making higher MK content to be not suitable for cement replacement since results in low cement strength. This observation corresponds with studies from other fields especially in concrete [32,39,52,53].

The replacement of OWC with MK10 contributes to strength evolution. However, CS lower than that of MK20 was observed especially at later curing age. The contribution to CS at late curing age particularly from 14 days to 28 days is due to pozzolanic reaction. The latter depends on the sufficient amount of MK available for reacting with CH from cement hydration. MK10 contributed less amount required to convert CH into secondary C-S-H gel at a later age compared to MK20. The figure also shows that replacing OWC with MK, the CS achieved optimization at 20%wt. The amount was sufficient for this study to give the highest strength both for early and later age. Both filler and pozzolanic reactions benefited the production of secondary C-S-H gel which added to cement strength for the MK20 mix. Although Albeit, MK30, and MK40 displayed low values of CS, they are significant alternatives for OWC replacement for properties improvement since both displayed strength which meets the cementing standard of 13 MPa [34].

3.3. Shear bond strength

Fig. 4 presents the results of SBS for the five mix ratios with MK0 representing the neat OWC. All mix proportions of the cement design with and without MK showed increasing trends of SBS with curing age. MK10 and MK20 had a better trend of the bond strength development as compared to MK0, MK30, and MK40 from the hydration age of 3 days, and kept increasing with time. The MK particles are better distributed in the mix and provide a better contribution to hydration products while consuming most of the CH formed from cement hydration. The contribution to strength evolution is due to the production of more hydration products through filler effect and pozzolanic reaction both at an early age and later age. The addition of calcium aluminate silicate hydrate (C-A-S-H) due to incorporation of the Alumina phase from MK dissolution into the C-S-H structure and pozzolanic reaction leads to the reduction of bulky CH. These reaction products reduce the harmful pores, thereby increasing the cement strength evolution. The reaction products also contribute to the strong bonding of the cement to the simulated sand rock formation.

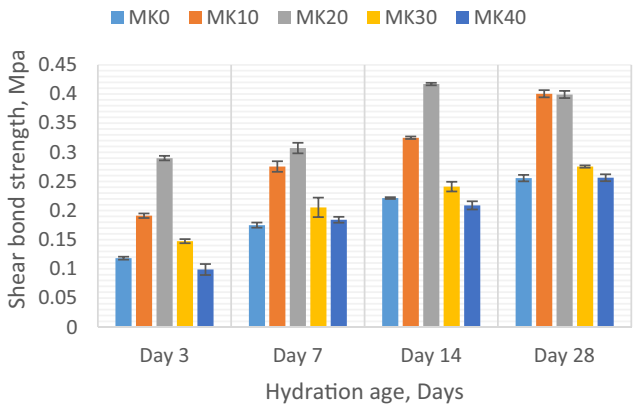

Fig. 4. Shear-bond strength (MPa) for different mixes with curing age (Days).

CHs are a weak form of hydration products since they are prone to dissolution. Their removal through reacting with smaller MK particles results in the addition of secondary C-S-H and C_2ASH_8 which significantly add to strength evolution [54,55]. Secondary hydrates take the place of consumed CH while allowing small particles of MK to fill the left harmful pores. MK30 and MK40 showed lower bond strength development than MK0, MK10, and MK20. The main reason for the low contribution is due to the dilution effect. The latter leads to the presence of an excess MK with no corresponding CH to react with. The dilution effect also leads to low cement availability; and low amount of C-S-H for strength evolution. As a result, the bulkiness does not significantly impact the rate of cement hydration and bond strength evolution. From the observation of each mix proportion, it is obvious that MK20 played a key role in strength evolution. It was a sufficient amount to convert the unstable form of CH into secondary C-S-H and C-A-S-H. C-A-S-H is formed due to the reactive Aluminates from MK dissolution. It polymerizes thereby increasing the volume of the hydration products in the cementitious system [24,56]. The volume increase of the hydrating cement due to C-S-H and C-A-S-H are important factors for increased SBS evolution. The presence of Aluminates in the binary system further serves the advantage of rapidly consuming gypsum. The consumption during the initial period of hydration further prevents the formation of ettringite which adversely affects the cement strength evolution. This is evident from the XRD data analyses where no ettringite was detected.

Consumption of CH along the cement-formation interface and increase in the hydrated structure are two possible means of increasing the SBS [2,57,58]. The existence of unreacted MK in the spaces between C-S-H phases might have contributed to the reduced strength for samples with higher MK content as compared to MK10 and MK20. Nevertheless, from this study, it is obvious that replacing OWC with MK can increase the bond strength and thus bring about the increased life of the oil and gas wells. Supplementing OWC with MK will equally cut down the energy required in cement production. It will further protect the environment from the effect of CO_2 greenhouse gas emitted from cement production.

3.4. XRD studies

Fig. 5 presents the XRD patterns for the selected mixes cured for 28 days. The patterns show higher peak intensities for neat OWC presented as MK0. It indicates the presence of high percentages

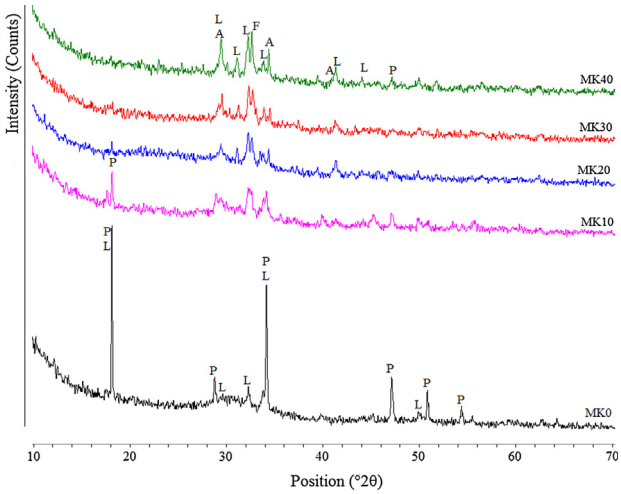

Fig. 5. XRD data of MK0, MK10, MK20, and MK30 at age of 28 days. The labeled picks are: P-Portlandites (Ca (OH)2); L-Calcium silicate (Ca2SiO4); A- Calcium silicate (Ca3SiO5); F- Calcium iron aluminate (Ca2FeAlO5).

of CH at a late age. This gives the evidence that cement hydration had proceeded to this late age. Although not detected for neat OWC, C-S-H has more contribution to strength evolution than CH. C-S-H hydration phase shows excellent physical and chemical stability at temperatures up to 110 °C beyond which cement strength decreases [11,34]. Their contribution to mechanical strength, therefore, depends on temperature and curing time out of other factors. Increasing the temperature of sample curing beyond 120 °C can compromise the strength evolution due to silicate hydrates phase changes. The formation of strength deteriorating crystalline silicates such as α-C_2S and $C_6S_2H_3$ results in a cement matrix with lower mechanical strength and higher permeability [19,59–61]. As can be seen from the fig, the two crystalline hydrates did not form until the time of the test due to the absence of favorable temperature for their formation. This means curing at a temperature of 80 °C did not favor the C-S-H phase change into α-C_2S and $C_6S_2H_3$. This is evident from the observed linear strength evolution for MK0 with curing time.

Since the majority of hydration products of MK are amorphous, they are often not detectable with XRD [24]. However, the intensities of the peaks corresponding to CH can be used to explain the status of cement hydration and strength evolution. Detected low CH intensity for MK binary systems reveals three insights: first, low hydration rate leads to fewer hydration products; the second reason is attached to the pozzolanic reaction of MK with CH to produce secondary C-S-H and C-A-S-H (not detected). This reduced the amount of CH to the time of the test while leading to strength evolution. The third reason is due to the dilution effect resulting from OWC replacement especially with higher MK dosage (MK30 and MK40). The replacement reduced the cement proportion resulting in low hydration products.

The binary system for MK10 and MK20 displayed lower peak intensities for both CH and Larnite. The observation can be attributed to the possibility that CH was mostly reacted to more hydrates to the age of 28 curing days. Therefore, some cement remained unreacted in the system to the later curing age which could bring more reaction with prolonged curing. The patterns for MK30 and MK40 showed no CH except some traces as all patterns analyzed depicted the presence of di-and tri-calcium silicates. The presence of traces of tri-calcium silicate and di-calcium silicates indicated the presence of unreacted cement. This is due to inhibition at some point by aluminate from MK dissolution, on the active surface of C-S-H which blocks the nucleation for further reaction. Therefore, the extended curing time of samples is recommended for the follow-up studies to know if a further contribution to strength can be observed.

3.5. TG-DSC studies

Fig. 6 presents the TG-DSC curves for selected samples with and without MK. The curves show mass and phase changes for MK0, MK10, and MK20 at different temperature ranges. Three major DSC endothermic peaks 90–120 °C, 130–160 °C and 441–452.7 °C can be identified. The first endothermic peak at 90–120 °C is attributed to dehydration of C-S-H while the second at 130–160 °C is attributable to dissociation of C-A-S-H. This gives evidence of cement hydration and pozzolanic reaction which added to the strength evolution. MK0 shows a high DSC peak value at 452.7 °C compared to MK10 and MK20 at 444.1 and 444.5 °C, respectively. This means MK0 had more CH compared to the MK binary systems. The decrease in CH for the binary systems is attributed to the conversion of CH into secondary C-S-H through a pozzolanic reaction. The observation corresponds with the XRD patterns that revealed the CH as evidence of cement hydration. Lower in CH amount means more C-S-H exist in the system which significantly adds to the cement strength. The TG curve indicates the percentage of

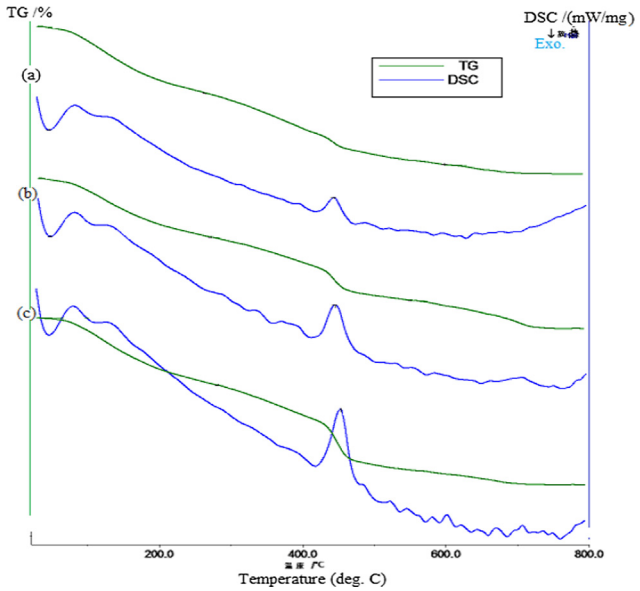

Fig. 6. TG-DSC curves: (a) MK20; (b) MK10; (c) MK0.

mass loss. It can be observed that the mass loss in the temperature range up to about 290 °C is attributed to the dehydration of silicate hydrates. The corresponding value for MK0, MK10, and MK20 are 7.13, 7.15 and 7.48%, respectively. The percentage of mass loss in the temperature range of 420 and 452.7 °C corresponds to the thermal degradation of CH [62]. Under this temperature range, CH decomposes into CaO and H_2O. Thus, the TG percentage of mass loss is due to the volatilization of H_2O [28]. The corresponding percentage mass loss due to CH decomposition for MK0, MK10, and MK20 is 11.75, 7.69 and 7.01%, respectively. This means the higher the percentage mass loss, the higher the calcium silicate hydrates formed during cement hydration for strength evolution.

3.6. Shear bond and compressive strength statistical significance

Two-way analysis of variance (ANOVA) and Tukey test were done to check whether the binary system with varying MK content is a statistically significant difference. The mean CS and SBS for each binary system and the reference sample generated by ANOVA were used to provide necessary information for comparison. The general population of samples was statistically significant since the overall *F* value was greater than the *Fcrit* with columns as the source of validation. It was also observed that the experimental *p*-value was less than the set alpha value (0.05). However, to compare the means of each treatment Tukey test was done. The absolute difference for each comparison was done while the critical value was calculated according to the equation; $Fcrit. = Q * Sqrt(MS/n)$. *Q* value was obtained from the score table based on treatments (k = 5), and error term (df). The number of treatments (n) for each of the system, MS and df values is as presented in ANOVA results (Table 3).

Table 4 presents the results for the Tukey test. From this table, it was observed that all treatments involving binary system and neat OWC have significance on CS except that there was no statistical difference between 30 and 40% of MK. As discussed in earlier sections, the higher content of MK has less effect on cement properties improvement. Thus, increasing MK content from 30 to 40% did not have a significant impact on the CS strength of the hydrated system. This is also evident on SBS as it was noticed that, replacement of OWC up to 40% was not significant for cement-formation bond strength. Therefore these statistics give an insight into optimizing MK content, not exceeding 30% for better oil and gas well cementing.

Table 3
ANOVA results.

Source of Variation	CS						SBS					
	SS	df	MS	F	P-Value	Fcrit.	SS	df	MS	F	P-Value	Fcrit.
Sample	1019.27	4	254.82	68.25	2.5E-17	2.61	0.256	4	0.064	402.90	9.9E-32	2.61
Columns	468.18	3	156.06	41.80	2.1E-12	2.84	0.189	3	0.063	396.35	9.0E-30	2.84
Interact	56.05	12	4.67	1.25	0.28	2.00	0.016	12	0.001	8.30	1.5E-07	2.00
Within	149.34	40	3.37	–	–	–	0.006	40	0.0002	–	–	–
Total	1692.85	59	–	–	–	–	0.466	59	–	–	–	–

Table 4
Tukey test results.

Comparisons (mean, Mpa)	CS			SBS		
	Absolute difference	Critical value	Comparison results	Absolute difference	Critical value	Comparison results
MK0 vs. MK10	2.326	2.253	√	0.105	0.015	√
MK0 vs. MK20	6.228	2.253	√	0.161	0.015	√
MK0 vs. MK30	4.342	2.253	√	0.161	0.015	√
MK0 vs. MK40	4.684	2.253	√	0.006	0.015	x
MK10 vs. MK20	3.902	2.253	√	0.055	0.015	√
MK10 vs. MK30	6.668	2.253	√	0.081	0.015	√
MK10 vs. MK40	7.010	2.253	√	0.187	0.015	√
MK20 vs. MK30	10.569	2.253	√	0.136	0.015	√
MK20 vs. MK40	10.912	2.253	√	0.136	0.015	√
MK30 vs. MK40	0.342	2.253	x	0.030	0.015	√

Note: √ = mean are significantly different; x = means are not significantly different.

4. Conclusion

Based on the objectives and findings of this study, the following conclusions are made.

- Metakaolin content affects the slurry workability, implying high water demand. As observed in this study, high metakaolin content requires more dispersant for slurry consistency.
- All the studied oil well cement replacements with metakaolin showed increasing trends of compressive and shear bond strengths with hydration age.
- Although there is a decreasing trend of compressive strength with high metakaolin dosage, all the studied mixes meet the basic standards of cementation.
- Metakaolin improves the shear bond strength and thus are promising materials to reduce the use of oil well cement while giving assurance of good integrity.
- Replacing oil well cement with metakaolin between 10 and 30% results in significant compressive and shear bond strengths. Additional field tests to accommodate the varying subsurface conditions in oil and gas wells for future use optimization is therefore recommended.

Overall, the results obtained from this study have provided new insight into the significance of incorporating metakaolin into cement as a step to having improved oil and gas well cement system for strong cement-formation interface bond. It further gives a solution to combating environmental problems due to CO_2 emission in cement production. However, prospective studies should be done to characterize microstructures formed at the cement-formation interface to enlighten the exact cause of bond strength due to an optimized metakaolin supplement.

Credit Author Statement

P. E. Mabeyo conceived and planned the experiment. **P. E. Mabeyo** and **Y. S. Ibrahim** performed the experiment, analyzed data and prepared the manuscript. **J. GU** supervised the research work, reviewed and edited the manuscript. All the three authors discussed the results and produced the last version of the manuscript. All authors read and approved the final manuscript.

Acknowledgments

Funding of this work was done by National Natural Science Foundation of China (grant no. 51774258 and 41972326), National Science and Technology Major Project of China (grant no. 2017ZX05009003-003), and Fundamental Research Funds for the Central Universities, China University of Geosciences (Wuhan) (grant no. CUGQYZX1710).

References

[1] J. Bårdsen, P. Hazel, R.R. Vasques, Ø. Hjorteland, Ø. ElKesKog, Improved zonal isolation in open hole applications, Soc. Pet. Eng. - SPE Bergen One Day Semin. 2014 (2014) 84–93.
[2] J. Hwang, R. Ahmed, S. Tale, S. Shah, Shear bond strength of oil well cement in carbonic acid environment, J. CO2 Util. 27 (2018) 60–72, https://doi.org/10.1016/j.jcou.2018.07.001.
[3] J. Plank, C. Tiemeyer, D. Buelichen, A study of cement/mudcake/formation interfaces and their impact on the sealing quality of oilwell cement, Soc. Pet. Eng. - IADC/SPE Asia Pacific Drill. Technol. Conf. 2014 Driv. Sustain. Growth Through Technol. Innov., 2014. 1–8.
[4] S. Salehi, M.J. Khattak, A.H. Bwala, F.S. Karbalaei, Characterization, morphology and shear bond strength analysis of geopolymers: Implications for oil and gas well cementing applications, J. Nat. Gas Sci. Eng. 38 (2017) 323–332, https://doi.org/10.1016/j.jngse.2016.12.042.
[5] R. Jadhav, V.G. Rao Palla, A. Datta, M. Dumbre, Effect of casing coating materials on shear-bond strength, Soc. Pet. Eng. – SPE/IATMI Asia Pacific Oil Gas Conf. Exhib. 2017 (2017) 17–19.
[6] K.M. Cowan, A.H. Hale, J.J. Nahm, Conversion of drilling fluids to cements with blast furnace slag: performance properties and applications for well cementing, Proc. - SPE Annu. Tech. Conf. Exhib. Delta (1992) 277–288.
[7] J. Gu, W. Qin, Experiments on integrated solidification and cementation of the cement-formation interface using the Mud Cake to Agglomerated Cake (MTA) method, Pet. Explor. Dev. 37 (2010) 226–231, https://doi.org/10.1016/S1876-3804(10)60028-6.
[8] J. Gu, H. Ju, Z. Su, X. Hu, H. Gao, B. Shen, Z. Deng, S. Tian, X. Yue, Q. Wang, D. Sun, W. Zhang, Solidifying mud cake to improve cementing quality of shale gas well: a case study, Open Fuels Energy Sci. J. 8 (2015) 149–154, https://doi.org/10.2174/1876973X01508010149.
[9] J. Gu, J. Huang, H. Hao, Influence of mud cake solidification agents on thickening time of oil well cement and its solution, Constr. Build. Mater. 153 (2017) 327–336, https://doi.org/10.1016/j.conbuildmat.2017.07.128.
[10] H. Hao, J. Gu, J. Huang, Z. Wang, Q. Wang, Y. Zou, W. Wang, Comparative study on cementation of cement-mudcake interface with and without mud-cake-

solidification-agents application in oil & gas wells, J. Pet. Sci. Eng. 147 (2016) 143–153, https://doi.org/10.1016/j.petrol.2016.05.014.
[11] P. Souza, R. Soares, M. Anjos, J. Freitas, A. Martinelli, D. Melo, Cement slurries of oil wells under high temperature and pressure: the effects of the use of ceramic waste and silica flour, Brazilian J. Pet. Gas. 6 (2012) 105–113, https://doi.org/10.5419/bjpg2012-0009.
[12] H. Liu, Y. Bu, S. Guo, Improvement of aluminium powder application measure based on influence of gas hole on strength properties of oil well cement, Constr. Build. Mater. 47 (2013) 480–488, https://doi.org/10.1016/j.conbuildmat.2013.05.057.
[13] S. Liu, D. Li, J. Yuan, F. Qi, J. Shen, M. Guo, Cement sheath integrity of shale gas wells: a case study from the Sichuan Basin, Nat. Gas Ind. B. 5 (2018) 22–28, https://doi.org/10.1016/j.ngib.2017.11.004.
[14] B. Lothenbach, K. Scrivener, R.D. Hooton, Supplementary cementitious materials, Cem. Concr. Res. 41 (2011) 1244–1256, https://doi.org/10.1016/j.cemconres.2010.12.001.
[15] A. Shahriar, M.L. Nehdi, Advances in Civil Engineering Materials Effect of Supplementary Cementitious Materials on Rheology of Oil Well Cement Slurries Effect of Supplementary Cementitious Materials on Rheology of Oil Well Cement Slurries, 3, 2014. doi: 10.1520/ACEM20120027.
[16] M.S. Amin, S.M.A. El-Gamal, S.A. Abo-El-Enein, F.I. El-Hosiny, M. Ramadan, Physico-chemical characteristics of blended cement pastes containing electric arc furnace slag with and without silica fume, HBRC J. 11 (2015) 321–327, https://doi.org/10.1016/j.hbrcj.2014.07.002.
[17] S.A. Abo-El-Enein, F.S. Hashem, M.S. Amin, D.M. Sayed, Physicochemical characteristics of cementitious building materials derived from industrial solid wastes, Constr. Build. Mater. 126 (2016) 983–990, https://doi.org/10.1016/j.conbuildmat.2016.09.112.
[18] S.M.A. El-Gamal, M.S. Amin, M. Ramadan, Hydration characteristics and compressive strength of hardened cement pastes containing nano-metakaolin, HBRC J. 13 (2017), https://doi.org/10.1016/j.hbrcj.2014.11.008. 144–121.
[19] M.S. Amin, A.O. Habib, S.A. Abo-El-Enein, Hydrothermal characteristics of high-slag cement pastes made with and without silica sand, Adv. Cem. Res. 24 (2012) 23–31, https://doi.org/10.1680/adcr.2012.24.1.23.
[20] A. Shvarzman, K. Kovler, G.S. Grader, G.E. Shter, The effect of dehydroxylation/amorphization degree on pozzolanic activity of kaolinite, Cem. Concr. Res. 33 (2003) 405–416, https://doi.org/10.1016/S0008-8846(02)00975-4.
[21] R. Mejía De Gutiérrez, J. Torres, C. Vizcayno, R. Castello, Influence of the calcination temperature of kaolin on the mechanical properties of mortars and concretes containing metakaolin, Clay Miner. 43 (2008) 177–183, https://doi.org/10.1180/claymin.2008.043.2.02.
[22] D.A. Sinha, Evaluation of metakaolin for use in concrete, Int. J. Sci. Res. Dev. 1 (2014) 3–5.
[23] S.A. Abo-El-Enein, M.S. Amin, F.I. El-Hosiny, S. Hanafi, T.M. ElSokkary, M.M. Hazem, Pozzolanic and hydraulic activity of nano-metakaolin, HBRC J. 10 (2014) 64–72, https://doi.org/10.1016/j.hbrcj.2013.09.006.
[24] M. Boháč, R. Novotný, J. Másilko, T. Opravil, F. Šoukal, R.S. Yadav, M. Palou, Hydration of synthetized clinker phases C_3S and C_3A with metakaolin in isothermal conditions, Adv. Mater. Res. 1124 (2015) 23–30, https://doi.org/10.4028/www.scientific.net/amr.1124.23.
[25] G.S. Barger, J. Bayles, B. Blair, D. Brown, H. Chen, T. Conway, P. Hawkins, Ettringite formation and the performance of concrete, Portl. Cem. Assoc. (2001) 1–16.
[26] D. da Silva Andrade, J.H. da Silva Rêgo, P.C. Morais, A.N. de Mendonça Lopes, M. F. Rojas, Investigation of C-S-H in ternary cement pastes containing nanosilica and highly-reactive supplementary cementitious materials (SCMs): microstructure and strength, Constr. Build. Mater. 198 (2019) 445–455, https://doi.org/10.1016/j.conbuildmat.2018.10.235.
[27] A. Kaur, V.P.S. Sran, Use of metakaolin as pozzolanic material and partial replacement with cement in concrete (M30), Asian Reviwe Mech. Eng. 5 (2016) 9–13.
[28] D. da Silva Andrade, J.H. da Silva Rêgo, P. Cesar Morais, M. Frías Rojas, Chemical and mechanical characterization of ternary cement pastes containing metakaolin and nanosilica, Constr. Build. Mater. 159 (2018) 18–26, https://doi.org/10.1016/j.conbuildmat.2017.10.123.
[29] J. Chen, S.C. Kou, C.S. Poon, Hydration and properties of nano-TiO2 blended cement composites, Cem. Concr. Compos. 34 (2012) 642–649, https://doi.org/10.1016/j.cemconcomp.2012.02.009.
[30] B. Ma, H. Li, X. Li, J. Mei, Y. Lv, Influence of nano-TiO2 on physical and hydration characteristics of fly ash–cement systems, Constr. Build. Mater. 122 (2016) 242–253, https://doi.org/10.1016/j.conbuildmat.2016.02.087.
[31] N.M. Al-Akhras, Durability of metakaolin concrete to sulfate attack, Cem. Concr. Res. 36 (2006) 1727–1734, https://doi.org/10.1016/j.cemconres.2006.03.026.
[32] H.M. Khater, Influence of metakaolin on resistivity of cement mortar to magnesium chloride solution, J. Mater. Civ. Eng. 23 (2011) 1295–1301, https://doi.org/10.1061/(ASCE)MT.1943-5533.0000294.
[33] A. Brandl, J. Cutler, A. Seholm, M. Sansil, G. Braun, Cementing solutions for corrosive well environments, SPE Drill. Complet. 26 (2011) 208–219, https://doi.org/10.2118/132228-PA.
[34] Y. Bu, J. Du, S. Guo, H. Liu, C. Huang, Properties of oil well cement with high dosage of metakaolin, Constr. Build. Mater. 112 (2016) 39–48, https://doi.org/10.1016/j.conbuildmat.2016.02.173.
[35] H. Becker, G. Peterson, Bond of Cement Composition for Cementing Wells, German, 1963
[36] L.G. Carter, G.W. Evans, A study of cement-pipe bonding, J. Pet. Technol. 16 (1964) 157–160, https://doi.org/10.2118/764-pa.
[37] W.G. Bearden, J.W. Spurlock, G.C. Howard, Control and prevention of inter-zonal flow, J. Pet. Technol. 17 (1965) 579–584, https://doi.org/10.2118/903-pa.
[38] F. Lagier, K.E. Kurtis, Influence of Portland cement composition on early age reactions with metakaolin, Cem. Concr. Res. 37 (2007) 1411–1417, https://doi.org/10.1016/j.cemconres.2007.07.002.
[39] P. Dinakar, P.K. Sahoo, G. Sriram, Effect of metakaolin content on the properties of high strength concrete, Int. J. Concr. Struct. Mater. 7 (2013) 215–223, https://doi.org/10.1007/s40069-013-0045-0.
[40] T.L. Weng, W.T. Lin, A. Cheng, Effect of metakaolin on strength and efflorescence quantity of cement-based composites, Sci. World J. 2013 (2013), https://doi.org/10.1155/2013/606524.
[41] A.A. Ramezanianpour, H. Bahrami Jovein, Influence of metakaolin as supplementary cementing material on strength and durability of concretes, Constr. Build. Mater. 30 (2012) 470–479, https://doi.org/10.1016/j.conbuildmat.2011.12.050.
[42] H. El-Diadamony, A.A. Amer, T.M. Sokkary, S. El-Hoseny, Hydration and characteristics of metakaolin pozzolanic cement pastes, HBRC J. 14 (2018) 150–158, https://doi.org/10.1016/j.hbrcj.2015.05.005.
[43] M.S. Morsy, Y.A. Al-Salloum, H. Abbas, S.H. Alsayed, Behavior of blended cement mortars containing nano-metakaolin at elevated temperatures, Constr. Build. Mater. 35 (2012) 900–905, https://doi.org/10.1016/j.conbuildmat.2012.04.099.
[44] J. Gu, P. Zhong, C. Shao, S. Bai, H. Zhang, K. Li, Effect of interface defects on shear strength and fluid channeling at cement-interlayer interface, J. Pet. Sci. Eng. 100 (2012) 117–122, https://doi.org/10.1016/j.petrol.2012.11.021.
[45] American Petroleum Institute, API Specification 10A – Specification for Cements and Materials for Well Cementing, 2002.
[46] American Petroleum Institute, Recommended Practice for Testing Well Cements, API Recommended Practice 10B-2 Second Edition, APRIL 2013 (R2019), 2013.
[47] H.K.J. Ladva, B. Craster, T.G.J. Jones, G. Goldsmith, D. Scott, The cement-to-formation interface in zonal isolation, SPE Drill. Complet. 20 (2005) 186–197, https://doi.org/10.2118/88016-PA.
[48] E. Pustovgar, R.K. Mishra, M. Palacios, J.B. d'Espinose de Lacaillerie, T. Matschei, A.S. Andreev, H. Heinz, R. Verel, R.J. Flatt, Influence of aluminates on the hydration kinetics of tricalcium silicate, Cem. Concr. Res. 100 (2017) 245–262, https://doi.org/10.1016/j.cemconres.2017.06.006.
[49] J. Lapeyre, H. Ma, A. Kumar, Effect of particle size distribution of metakaolin on hydration kinetics of tricalcium silicate, J. Am. Ceram. Soc. (2019) 5976–5988, https://doi.org/10.1111/jace.16467.
[50] R. Siddique, J. Klaus, Influence of metakaolin on the properties of mortar and concrete: a review, Appl. Clay Sci. 43 (2009) 392–400, https://doi.org/10.1016/j.clay.2008.11.007.
[51] A. Kumar, T. Oey, G. Falzone, J. Huang, M. Bauchy, M. Balonis, N. Neithalath, J. Bullard, G. Sant, The filler effect: the influence of filler content and type on the hydration rate of tricalcium silicate, J. Am. Ceram. Soc. 100 (2017) 3316–3328, https://doi.org/10.1111/jace.14859.
[52] S. Wild, J.M. Khatib, A. Jones, Relative strength, pozzolanic activity and cement hydration in superplasticised metakaolin concrete, Cem. Concr. Res. 26 (1996) 1537–1544, https://doi.org/10.1016/0008-8846(96)00148-2.
[53] X.Y. Wang, R. Gupta, Analysis of hydration and optimal strength combinations of cement-limestone-metakaolin ternary composite, Adv. Mater. Sci. Eng. 2019 (2019), https://doi.org/10.1155/2019/8361810.
[54] M.F. Rojas, J. Cabrera, The effect of temperature on the hydration rate and stability of the hydration phases of metakaolin-lime-water systems, Cem. Concr. Res. 32 (2002) 133–138, https://doi.org/10.1016/S0008-8846(01)00642-1.
[55] M.F. Rojas, M.I. Sánchez de Rojas, The effect of high curing temperature on the reaction kinetics in MK/lime and MK-blended cement matrices at 60 °C, Cem. Concr. Res. 33 (2003) 643–649, https://doi.org/10.1016/S0008-8846(02)01040-2.
[56] A.F. Jamsheer, K. Kupwade-Patil, O. Büyüköztürk, A. Bumajdad, Analysis of engineered cement paste using silica nanoparticles and metakaolin using 29Si NMR, water adsorption and synchrotron X-ray Diffraction, Constr. Build. Mater. 180 (2018) 698–709, https://doi.org/10.1016/j.conbuildmat.2018.05.272.
[57] M.N. Al Khalaf, C.L. Page, Steel/mortar interfaces: microstructural features and mode of failure, Cem. Concr. Res. 9 (1979) 197–207, https://doi.org/10.1016/0008-8846(79)90026-7.
[58] P.A. Parcevaux, P.H. Sault, Cement shrinkage and elasticity: a new approach for a good zonal isolation, Proc. – SPE Annu. Tech. Conf. Exhib. (1984-Septe (1984).
[59] L.H. Eilers, R.L. Root, Long-term effects of high temperature on strength retrogression of cements, Soc. Pet. Eng. - Fall Meet. Soc. Pet. Eng. AIME, FM 1974 (1974) 1–11, https://doi.org/10.2523/5871-ms.
[60] A.C. Jupe, A.P. Wilkinson, K. Luke, G.P. Funkhouser, Class H cement hydration at 180 °C and high pressure in the presence of added silica, Cem. Concr. Res. 38 (2008) 660–666, https://doi.org/10.1016/j.cemconres.2007.12.004.
[61] M. Palou, V. Živica, T. Ifka, M. Boháč, M. Zmrzlý, Effect of hydrothermal curing on early hydration of G-Oil well cement, J. Therm. Anal. Calorim. 116 (2014) 597–603, https://doi.org/10.1007/s10973-013-3511-7.
[62] S.M.A. El-Gamal, S.A. Abo-El-Enein, F.I. El-Hosiny, M.S. Amin, M. Ramadan, Thermal resistance, microstructure and mechanical properties of type I Portland cement pastes containing low-cost nanoparticles, J. Therm. Anal. Calorim. 131 (2018) 949–968, https://doi.org/10.1007/s10973-017-6629-1.